Analysis of current–voltage measurements on Au/Ni/n-GaN Schottky contacts in a wide temperature range

W. Mtangi *, P.J. Janse van Rensburg, M. Diale, F.D. Auret, C. Nyamhere, J.M. Nel, A. Chawanda

University of Pretoria, Physics Department, Pretoria 0002, South Africa

ARTICLE INFO

ABSTRACT

Current–voltage characteristics of Au/Ni/n-GaN Schottky contacts have been measured in the 60–320 K temperature range. The zero bias barrier height, ϕ_{bo} and ideality factor, n have been studied as a function of temperature. The sharp increase in ideality factor at low temperatures has been explained as an effect of thermionic field emission. The deviation of the characteristics from the ideal thermionic behaviour is more pronounced with a decrease in temperature, in which the results obtained indicate the presence of other current transport mechanisms in the 60–280 K temperature range and the dominance of pure thermionic emission current at 300 K. The increase in barrier height with increasing temperature has been explained as an effect of barrier inhomogeneities.

© 2010 Elsevier B.V. All rights reserved.

1. Introduction

Study of wide band gap materials for applications in low temperature environments, e.g. satellites as well as high temperature environments of late has been of vast interest. Having a wide, direct band gap and good transport properties, GaN is ideally suited for intrinsic ultraviolet, UV detectors with high responsivities for wavelengths shorter than 365 nm [1]. The electrical characteristics of the GaN devices under these different temperature conditions are essential. GaN also has potential applications in optoelectronic devices operative in the spectral range from blue to UV. Electrical characteristics of metal contacts to n-GaN under different temperature conditions have been studied by many research groups [1–3]. Published reports indicate a barrier height of between 0.53 and 1.03 eV which is dependent on the types of metals used. Guo et al. [2] reported a room temperature barrier height of 0.66 eV on Ni Schottky contacts using the IV method, while a barrier height of 0.84 eV was also measured by Hacke et al. [3] on Au Schottky contacts by using the IV technique. Temperature dependent IV characteristics of metal Schottky contacts on n-GaN have been studied by many researchers in different temperature ranges. Dogan et al. [1] performed measurements on Au/Ni/n-GaN Schottky contacts in the 40–320 K temperature range. Their results indicate the variation in the IV characteristics in three different regions, with thermionic emission being the dominant transport mechanism.

From their report, they revealed the variation of the Richardson constant within these regions. Donoval et al. [4] also studied the IV characteristics of GaN Schottky contacts in the 125–300 K temperature range while Schmitz et al. [5] studied the IV characteristics of the Pd/GaN Schottky contacts up to 500 °C. In all their reports, they have reported the dependence of the barrier height and ideality factor on temperature. However, none of them reported about the variation of the observed leakage currents with temperature. In this paper, we have studied the IV characteristics of Au/Ni/n-GaN Schottky contacts in the 60–320 K temperature range and analysed the data by incorporating other current transport mechanisms and fitting the intermediate region of the IV curves to pure thermionic emission.

2. Experiment

GaN samples with a carrier concentration of 8.79×10^{17} cm^{-3} and resistivity of 7.93×10^{-2} Ω cm at room temperature as determined from Hall measurements supplied by TDI were used in this study. The samples were boiled in TCE for 5 min, boiled in isopropanol for another 5 min, boiled in aqua regia HCl:HNO$_3$ (1:5) for 10 min and rinsed in isopropanol. Etching HCl:H$_2$O (1:1) was performed for 1 min. After etching, the samples were blown dry using nitrogen gas. Ohmic contacts with composition Ti/Al/Ni/Au with thicknesses 15/220/40/50 nm were deposited using electron beam deposition at a pressure of approximately 1×10^{-7} Torr (at the four corners of the wafer). The samples were then annealed at a temperature of 500 °C for 5 min under argon atmosphere. Prior to Schottky contact deposition, the samples were rinsed in dilute HCl for 1 min and blown dry using nitrogen gas. Ni/Au Schottky contacts with

* Corresponding author at: University of Pretoria, Physics Department, 5-6 NW1 Building, Lynnwood Road Hatfield, Pretoria 0002, Gauteng, South Africa.
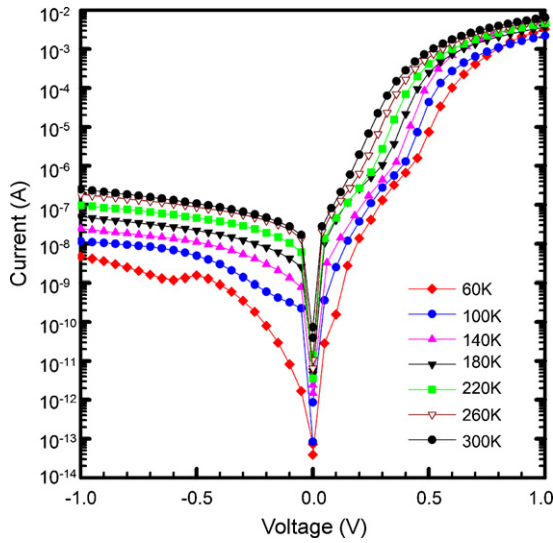E-mail address: wilbert.mtangi@up.ac.za (W. Mtangi).

Fig. 1. Temperature dependent semilogarithmic IV plot for the as-deposited Au/Ni/n-GaN Schottky diode in the 60–300 K range.

Fig. 2. Variation of the ideality factor (red circles) and barrier height (blue triangles) as with temperature. (For interpretation of the references to color in this figure legend, the reader is referred to the web version of the article.)

thicknesses 100/100 nm and diameter 0.6 mm were then resistively evaporated at a pressure of approximately 1×10^{-6} Torr. Temperature dependent IV measurements were performed in a closed cycle He cryostat in the 60–320 K temperature range.

3. Results and discussions

Room temperature IV measurements performed on the Schottky contacts reveal an average barrier height of (0.70 ± 0.01) eV, an average ideality factor of (1.23 ± 0.01) and an average reverse leakage current of $(1.1 \pm 0.1) \times 10^{-7}$ A (at $V = -1$ V). The series resistance has also been obtained as $(60 \pm 5)\,\Omega$ at room temperature. Fig. 1 shows the semilogarithmic IV characteristics of the Schottky contacts in the 60–320 K temperature range. 5–6 orders of rectification have been obtained from room temperature to 60 K. The IV characteristics of the contacts could not be determined below 60 K as the freeze out region was observed just below 60 K. The leakage current has been observed to decrease with decreasing temperature. It can be clearly seen that at low temperatures, i.e. below 300 K, the curves indicate the presence of other current transport mechanisms other than thermionic emission. The IV curves within the temperature range 60–280 K can be fitted to two linear regions with the lower region being fitted to generation recombination while the intermediate region fits to pure thermionic emission [6]. The upper part of the curves which shows deviation from linearity defines the series resistance. The generation/recombination effects within the 60–280 K temperature range indicate a strong dependence on temperature and bias. Considering the 60 K temperature curve, the effects of generation/recombination are pronounced for voltages ≤ 0.5 V. As the temperature increases, the voltage range in which the effects of generation/recombination are defined decreases. At low temperatures the current through the diode is the sum of the thermionic current and generation recombination current with the generation/recombination current being dominant. The presence of generation/recombination current indicates the presence of defects in the GaN material that act as generation/recombination centres that trap carriers as they try to tunnel through the depletion region. Auret et al. [7] observed two defects with energy levels 0.27 and 0.61 eV in GaN grown by organometallic vapour phase epitaxy (OMVPE) while similar defects with same energy levels were obtained by Hacke et al. [8] in GaN grown by hydride vapour phase epitaxy using DLTS measurements. These defects are said to have been introduced during growth. We speculate that the GaN mate-
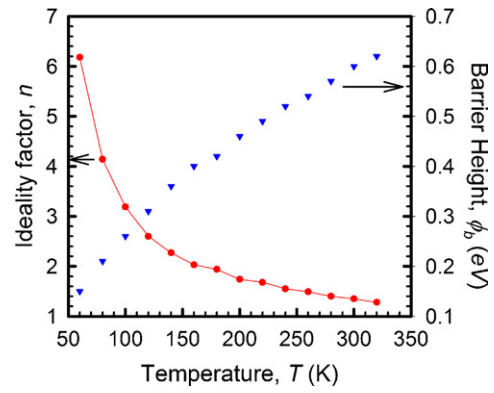
rial also contains these natural defects introduced during material growth. At high temperatures, with even low biases, the thermionic current dominates the generation recombination effects as carriers will be having enough energy to surpass the barrier. The current through the barrier of a Schottky contact (from the semiconductor into the metal), assuming pure thermionic emission is given by [6],

$$I = I_s \left\{ \exp\left(\frac{qV}{kT}\right) - 1 \right\} \tag{1}$$

where I is the current flowing through the diode in forward bias, I_s is the saturation current measured at zero bias, q is the electronic charge, V is the applied voltage, k is the Boltzmann constant and T is the Kelvin temperature. This approximation factors out the effects of the series resistance, R_s and the ideality factor n. Incorporating other current transport mechanisms and making the diode non-ideal, i.e. $n > 1$, the series resistance and the ideality factor need to be taken into account in Eq. (1) [9]:

$$I = I_s \exp\left[\frac{q(V - IR_s)}{nkT}\right] \left\{ 1 - \exp\left(-\frac{q(V - IR_s)}{kT}\right) \right\} \tag{2}$$

The ideality factor n is obtained from the slope of the semilogarithmic IV plot by fitting to the linear intermediate region and is given by [6,10],

$$\frac{1}{n} = \frac{kT}{q}\frac{d(\ln J)}{dV} \tag{3}$$

The saturation current is obtained as the intercept on the I axis after fitting to the intermediate linear region of the IV curves of Fig. 1 which resembles thermionic emission and is given by [10],

$$I_s = AA^*T^2 \exp\left(\frac{-q\phi_{b0}}{kT}\right) \tag{4}$$

where A is the Schottky contact cross-sectional area, A^* is the Richardson constant, ϕ_{b0} is the zero bias barrier height. Values of the ideality factors and the barrier heights obtained by making use of Eqs. (3) and (4), respectively are shown in Fig. 2 as a function of temperature. The barrier height increases with increasing temperature. Such a trend has been observed also by some researchers [1,4,5] on contacts deposited on GaN while [13] observed this trend on contacts deposited on Si. This increase in barrier height with increasing temperature has been explained as an effect of the barrier height being non-homogeneous, i.e. the barrier consists of low barrier embedded on a uniform barrier with individual cross-sectional areas. The existence of laterally extended Schottky barrier height (SBH) inhomogeneities at the metal–semiconductor (MS) interface allows for electron transport to be treated by the parallel conduction model [11,12]. Under this situation, the current flowing through the barrier is assumed to be the sum of all the individual
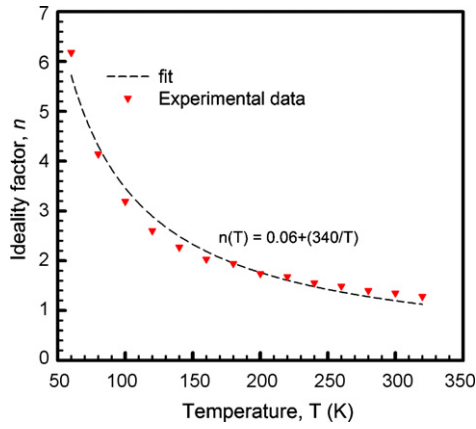
Fig. 3. Ideality factor, red triangles showing experimental values obtained using Eq. (3) as a function of temperature with the fit (dashed line) that best describes the variation of ideality with temperature. (For interpretation of the references to color in this figure legend, the reader is referred to the web version of the article.)
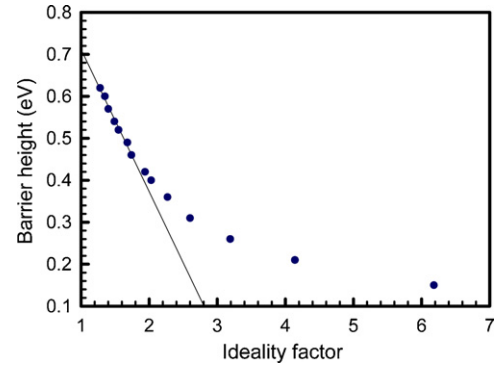

Fig. 4. Variation of barrier height with ideality factor to obtain the homogeneous barrier height at $n = 1$.

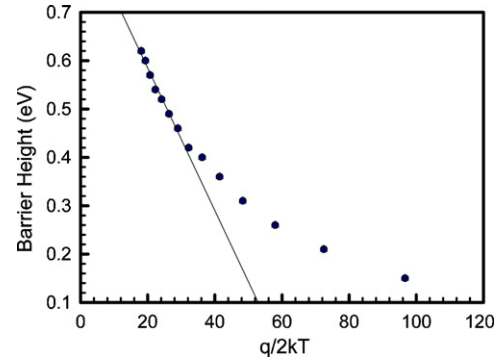**Fig. 5.** Variation of barrier height with temperature to obtain the mean barrier height and standard deviation as according to Eq. (6).

currents, I_i flowing through individual patches, each of its own area A_i and Schottky barrier height, Φ_i [12]:

$$I(V) = \sum I_i = A^* T^2 \left[\exp \left(\frac{qV}{kT} \right) - 1 \right] \sum \exp \left(\frac{-q\Phi_i}{kT} \right) A_i \qquad (5)$$

The current in this case will be dominated by the low barrier regions as at low temperatures, carriers will not be having enough energy to cross over the high barrier regions and thus the measured zero bias barrier height is low at low temperatures. The ideality factor increases with decreasing temperature. The values of the ideality factor in Fig. 2 were obtained by assuming pure thermionic emission, i.e. by evaluating the gradient of the intermediate region of the IV curves in the 60–320 K temperature range. Similar variations of the ideality factor with temperature have been observed by many researchers on different semiconductor material. The majority of them have attributed and explained it as an effect of the so-called T_0 anomaly, in which the ideality factor, $n(T)$ follows the relationship $n(T) = 1 + (T_0/T)$, where T_0 is a constant, independent of temperature [13]. From Fig. 2, the ideality factor increases sharply with decreasing temperature, indicating the presence of thermionic field emission (TFE) at low temperatures [14] other than the pure thermionic emission. As a result of this increase in ideality factor, the graph of T_0 as a function of temperature failed to yield a straight line as was noted by [13]. Thus the ideality factor obtained can fit well to $n(T) = 0.06 + (340/T)$ as shown in Fig. 3. The high values of the carrier density as measured by Hall Effect measurements at low temperatures supports the argument that tunneling of carriers through edge dislocations is the most favourable transport mechanism resulting in TFE instead of pure thermionic emission [15]. The dominance of thermionic field emission at low temperatures can also be explained by considering the results of Fig. 4. The variation of barrier height with ideality factor shows linearity at high temperatures, showing the existence of barrier inhomogeneities with a homogeneous barrier height of approximately 0.71 eV for an ideality factor, $n = 1$. Though inhomogeneities can also explain the increase in barrier height with temperature, the effects of high values of carrier concentration as from TDH measurements cause the tunneling of carriers and hence thermionic field emission to dominate at low temperatures. Assuming that at high temperatures, the barrier height follows a Gaussian spatial distribution of barrier heights around zero bias of mean value $\overline{\Phi}_{0Bn}$ and zero bias standard deviation σ_{0s}, the barrier height of the spatial inhomogeneous Schottky contact will have a temperature dependence given by the Werner–Guttler model [16]:

$$\Phi_{0Bn} = \overline{\Phi}_{0Bn} - \frac{\sigma_{0s}^2}{2k_B T} \qquad (6)$$

where Φ_{0Bn} is the apparent Schottky barrier height measured experimentally at 0 V, k_B is the Boltzmann constant and T is the temperature in K. A plot of Eq. (6) shown in Fig. 5 which reveals linearity in the high temperature region and deviation from linearity at low temperatures. From Fig. 5, the mean barrier height as been measured as 0.88 and 0.12 eV in the 140–300 K temperature region.
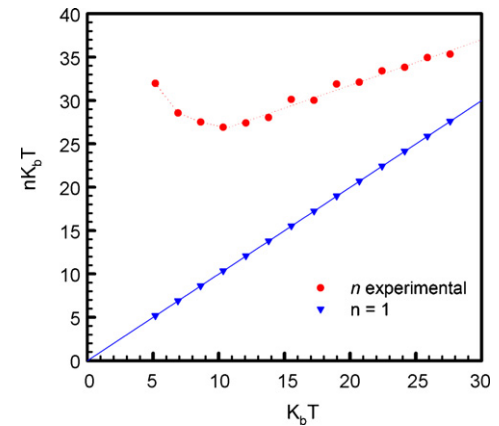

Fig. 6. Experimentally observed temperature dependence of the ideality factor (red circles) and the ideal situation, $n = 1$ (blue triangles) to determine the current transport mechanism of the Au/Ni/n-GaN contacts according to [15]. (For interpretation of the references to color in this figure legend, the reader is referred to the web version of the article.)

To further demonstrate the existence of thermionic field emission in the IV characteristics of the Schottky contacts, a plot of nk_bT against k_bT shown in Fig. 6 has been plotted. Results of Fig. 6 for n experimental show the temperature independence of the nk_bT against k_bT slope at low temperatures indicating the presence of TFE as interpreted by Saxena [17] relating the ideality factor to the different conduction mechanisms. Thus the large ideality factor values for the 60–120 K temperature range indicate the dominance of TFE within the Schottky contacts at low temperatures.

4. Conclusion

The current–voltage characteristics of the Au/Ni/n-GaN Schottky contacts in the 60–320 K temperature range have been successfully determined. At low temperatures, 60–120 K from the nk_bT versus k_bT plot the ideality factor values indicate the existence of thermionic field emission together with generation recombination. As temperature increases from 120 K up to 280 K the dependence of the slope of Fig. 6 on temperature indicates that thermionic emission starts to dominate, together with generation recombination. The variation of the barrier height at high temperatures as revealed by the linearity of the barrier height, ideality factor plot is due to barrier inhomogeneities at the MS contact. A homogeneous barrier height of 0.71 eV extrapolated to $n = 1$ has been measured within the 140–300 K temperature region. The quality of the contacts and observed low leakage current at $V = -1$ V has been attributed to the cleaning procedure used in sample preparation prior to Schottky contact deposition.

References

[1] S. Dogan, S. Duman, B. Gurbulak, S. Tuezemen, H. Morkoc, Phys. E 41 (2009) 646–651.
[2] J.D. Guo, F.M. Pan, M.S. Feng, R.J. Guo, P.F. Chou, C.Y. Chang, J. Appl. Phys. 80 (3) (1996).
[3] P. Hacke, T. Detchprohm, K. Hiramatsu, N. Sawaki, Appl. Phys. Lett. 63 (2676) (1993).
[4] D. Donoval, V. Kulikov, P. Beno, J. Racko, ASDAM 2002 Smolenice Castle, Slovakia, October, 2002.
[5] A.C. Schmitz, A.T. Ping, M.Asif. Khan, Q. Chen, J.W. Yang, I. Adesida, Electron. Lett. 32 (19) (1996).
[6] E.H. Rhoderick, R.H. Williams, Metal–Semiconductor Contacts, 2nd ed., Claredon Press, Oxford, 1988.
[7] F.D. Auret, S.A. Goodman, F.K. Koschnick, J.M. Spaeth, B. Beaumont, P. Gibart, Appl. Phys. Lett. 73 (25) (1998).
[8] P. Hacke, T. Detchprohm, K. Hiramatsu, N. Sawaki, K. Tadatomo, K. Miyake, J. Appl. Phys. 76 (304) (1994).
[9] D. Donoval, M. Barus, M. Zdimal, Solid State Electron 34 (1991) 1365.
[10] D.K. Schroder, Semiconductor Material and Device Characterization, 2nd ed., Wiley, New York, 1998.
[11] R.T. Tung, Appl. Phys. Lett. 58 (24) (1991).
[12] R. Singh, S.K. Arora, R. Tyagi, S.K. Agarwal, D. Kangilal, Bull. Mater. Sci. 23 (6) (2000).
[13] M. Mamor, A. Sellai, K. Bouziane, S.H. Al Harthi, M. Al Busaidi, F.S. Gard, J. Phys. D: Appl. Phys. 40 (2007) 1351–1356.
[14] R.T. Tung, Mater. Sci. Eng. R 35 (2001) 70.
[15] M. Mamor, J. Phys.: Condens. Matter 21 (2009) 335802.
[16] J.H. Werner, H.H. Guttler, J. Appl. Phys. 69 (1991) 1522.
[17] A.N. Saxena, Surf. Sci. 13 (1969) 151.